ACS Catalysis

Letter

pubs.acs.org/acscatalysis

Ni–Fe–S Cubanes in CO_2 Reduction Electrocatalysis: A DFT Study

J. B. Varley,*[,†,‡] H. A. Hansen,[†] N. L. Ammitzbøll,[¶] L. C. Grabow,[†,§] A. A. Peterson,[†,∥] J. Rossmeisl,[¶] and J. K. Nørskov*[,†,⊥]

[†]Department of Chemical Engineering, Stanford University, Stanford, California 94305-5025, United States

[‡]Lawrence Livermore National Laboratory, Livermore, California 94550, United States

[¶]Center for Atomic-Scale Materials Design, Department of Physics, Technical University of Denmark, DK-2800 Lyngby, Denmark

[§]Department of Chemical and Biomolecular Engineering, University of Houston, Houston, Texas 77204, United States

[∥]School of Engineering, Brown University, Providence, Rhode Island 02912, United States

[⊥]SUNCAT Center for Interface Science and Catalysis, Photon Science, SLAC National Accelerator Laboratory, Menlo Park, California 94025, United States

Supporting Information

ABSTRACT: In this work, we perform extensive mechanistic studies of CO_2 (electro)reduction by analogs to the active sites of carbon monoxide dehydrogenase (CODH) enzymes. We explore structure–property relationships for different cluster compositions and interpret the results with a model for CO_2 electroreduction we recently developed and applied to transition metal catalysts. Our results validate the effectiveness of the CODH in catalyzing this important reaction and give insight into why specific cluster compositions were adopted by nature.

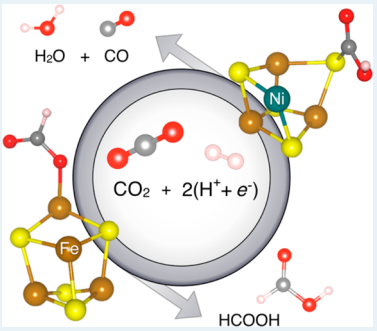

KEYWORDS: *electrochemistry, biocatalysis, carbon dioxide, carbon monoxide, density functional theory, iron, sulfur, nickel, dehydrogenase*

Chemical fuels, particularly hydrocarbons, provide energy storage densities far greater than the best batteries, capacitors, and mechanical storage means.[1] One way to provide a sustainable source of chemical fuels is artificial photosynthesis, in which CO_2 is reduced photocatalytically. Alternatively, if electrocatalytic CO_2 reduction is coupled to a carbon-neutral energy source, such as wind, solar, geothermal or hydroelectric, the overall production and combustion cycle of the chemical fuel can be CO_2-neutral. Certain electrocatalysts, such as Cu, have been shown to be capable of reducing CO_2 directly to the hydrocarbons methane and ethylene. However, they do so with quite poor efficiency, requiring about 1 V of overpotential for this process.[2,3]

Producing CO can be a first step toward chemical fuels and can be achieved through the reverse water-gas shift reaction or electrochemical CO_2 reduction.[4,5] For the latter, the production of CO should be thermodynamically downhill at a standard potential of −0.10 V versus the reversible hydrogen electrode (RHE), with an additional system-dependent overpotential required to drive the reaction. At present, noble metal electrocatalysts have come the closest to this limit, with Au-based catalysts in aqueous solution achieving overpotentials near −0.30 V at a current density of 0.2 $mA{\cdot}cm^{-2}$.[6] Once produced, CO can then be reacted in a Fischer–Tropsch synthesis to produce the desired hydrocarbons.

In nature, there exists a group of enzymes, carbon monoxide dehydrogenase (CODH), that have been shown to efficiently and reversibly catalyze the reduction of CO_2 to CO.[7] Two principal classes of CODH have been identified: Mo-$[Fe_4S_4]$-FAD CODHs from aerobic bacteria and Ni-$[Fe_4S_4]$-CODHs from anaerobic bacteria and archaea.[8] The Mo-CODHs have the advantage of not being sensitive toward oxygen, as opposed to the Ni-CODHs, but have a low turnover frequency compared with the Ni-CODHs.

Recently, a model was proposed of the electrochemical CO_2 to CO reduction process that captures the trends exhibited by both metals and the more active Ni-CODH enzymes.[9] The model, based on density functional theory (DFT) calculations, provides criteria for the catalytic activity as a function of the bond energies of the intermediates of the CO_2 electroreduction, COOH* and CO*. As an extension to this model,[9] we investigate a class of cubanes modeled after the Ni-CODH to further address how structure can correlate with catalytic activity. Our results suggest that cubanes can exhibit more favorable activity trends than those predicted for transition

Received: July 11, 2013
Revised: September 4, 2013
Published: October 11, 2013

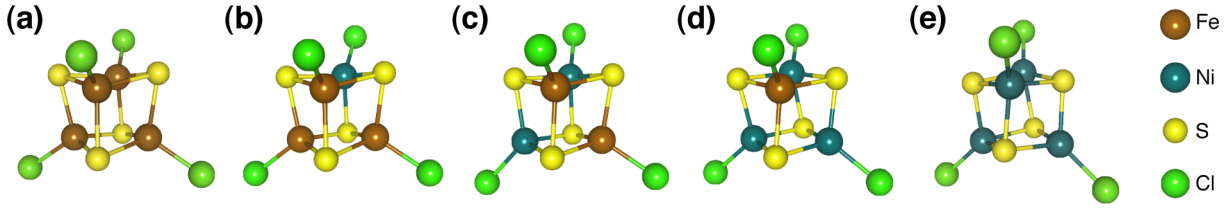

Figure 1. The investigated cubane model structures ranging from the all-iron cubane $[Fe_4S_4]$ (a) to the all-nickel cubane $[Ni_4S_4]$ (e).

metal elements[9] and also offer insight into the most active and most selective compositions of Ni−Fe clusters.

In the Ni-CODH enyzmes, the C cluster is widely accepted as being the active site of the CO_2/CO redox chemistry.[10] Depending on the bacterium, the active site exists in slightly different variations.[11] The variations all consist of a single Ni atom along with a number of Fe and S atoms arranged in an asymmetric heteronuclear cluster, all of which resemble a four-metal $[NiFe_3S_4]$ cubane structure with either an additional mononuclear or binuclear site coming off the cubane-like structure. Because the cubane-like structure is the same for the different variations of the active site, model structures inspired by the active site are chosen to investigate the catalytic activity of a set of Ni- and Fe-containing cubanes.

The physical structure of the clusters under investigation is a cube with metal, either Fe or Ni, and S atoms at alternating vertices. To understand the chemistry that occurs in these cubane-type structures and the effect of the substitution of a Ni atom for an Fe atom within the cubane, we have conducted computational studies of five different cubane structures, $[Fe_4S_4]$, $[NiFe_3S_4]$, $[Ni_2Fe_2S_4]$, $[Ni_3FeS_4]$, and $[Ni_4S_4]$, which are shown in Figure 1. As a base system, a $[Fe_4S_4]$ cubane was constructed, anchored by bonds to four Cl atoms in place of the cysteine linkages present in the biological system. This exact cubane structure is a stable, well-described structure that can be synthesized, which is why it was chosen as the base system.[12,13] Because the synthesized $[Fe_4S_4]$ cubanes have a charge of −2,[12] all clusters were modeled with an overall charge ranging from 0 to −2. The $[Ni_xFe_{4-x}S_4]$ (x = 0, ..., 4) cubanes are constructed by successively substituting a Ni atom for an Fe atom within the base cubane structure and reoptimizing the structure.

The catalytic activity of the model catalysts was investigated using DFT calculations in which the structure of each cubane was optimized in configurations without adsorbates and also with the possible reaction intermediates bound at the various binding sites. Because of the structural differences in the studied cubanes, we find the oxophilicity of the local environment of the COOH* and CO* adsorbates leads to distinct binding energies, and thus, distinct catalytic activities, that can deviate from the predicted scaling of transition metals.[5] This is manifested in the preferred binding sites for each intermediate: we find COOH* most favorably binds on S for all studied compositions, whereas OCHO* and CO* are most favorably adsorbed on a metal site. Interestingly, the COOH* do not prefer to bind to a Ni site, as previously found in some CODH enzymes,[9] highlighting the distinct structure−property relationships exhibited by cubanes of different geometries, compositions, and chemical environments. We find similar trends for all of the studied charge states, while the −2 charge state is predicted to be the most active overall. Full computational details are available in the Supporting Information.

The two-electron reduction of CO_2 can competitively form CO or HCOOH.

$$CO_2 + 2H^+ + 2e^- \rightarrow CO + H_2O \quad (1)$$

$$CO_2 + 2H^+ + 2e^- \rightarrow HCOOH \quad (2)$$

The calculated free energy diagrams for the lowest-energy pathways in the reduction of CO_2 to CO and HCOOH represented by eqs 1−2 are summarized in Figure 2 for the

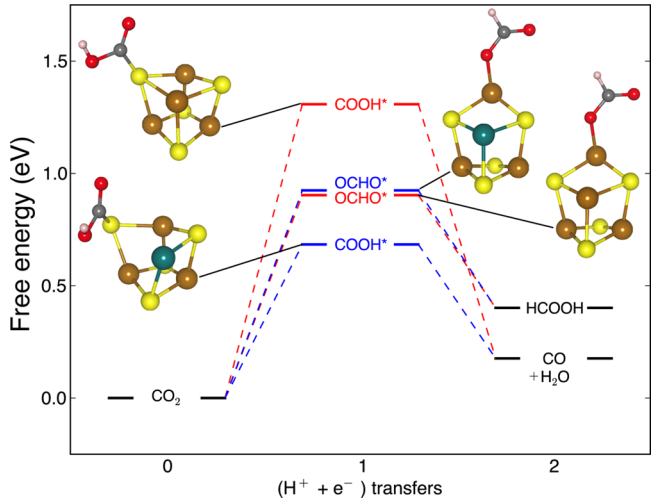

Figure 2. Free energy diagram for the reduction of CO_2 to HCOOH and CO on the $[Fe_4S_4]^{-2}$ (red) and $[NiFe_3S_4]^{-2}$ (blue) cubanes. The OCHO* intermediate, and thus, HCOOH formation, is favored by $[Fe_4S_4]^{-2}$, whereas $[NiFe_3S_4]^{-2}$ favors the formation of CO via the COOH* intermediate. CO* is less favorable than desorbed CO for both cubanes. For clarity, the terminating Cl atoms part of the model cubane clusters is not included in the insets.

$[Fe_4S_4]$ and $[NiFe_3S_4]$ cubanes, shown at 0 V vs RHE. The intermediate structure in the formation of HCOOH is found to be a formate (OCHO*) adsorbed monodentate on one of the metal atoms, as also depicted in Figure 2. The intermediate structure for the formation of CO is a carboxyl (COOH*), which adsorbs preferentially on a S atom in all Ni-containing cubanes (see Figure 2). Carboxyl can adsorb equally strong on an Fe or S atom only on the $[Fe_4S_4]$ cubane, indicating that the presence of Ni does alter the chemical environment in the COOH* binding. We note that adsorbed CO (CO*) and HCOOH (HCOOH*) are not favorable for any of the cubane compositions and will desorb under the ambient conditions used for the calculated free energies. Although it is also possible for COOH* to form HCOOH, we find this pathway is less thermodynamically favorable than the path to CO.

As can be seen in Figure 2 for the $[NiFe_3S_4]$, carboxyl adsorption on a Ni-containing cubane causes the Ni−S bond to

dx.doi.org/10.1021/cs4005419 | ACS Catal. 2013, 3, 2640−2643

break in the $[Ni_xFe_{4-x}S_4]$ cubane structures, leading to a stronger binding of COOH* to the cluster. Similarly, the adsorption of formate on an Fe site in the $[Fe_4S_4]$ and $[NiFe_3S_4]$ clusters causes the Fe−S bond to break, also stabilizing the OCHO* intermediate for the composition with two or fewer Ni atoms. In general, we find that this opening of the cluster leads to a much larger stabilization of the COOH* intermediate relative to the OCHO*, resulting in a major qualitative change in the reduction pathways. This can be seen in Figure 3, where we plot the binding energies of the COOH*

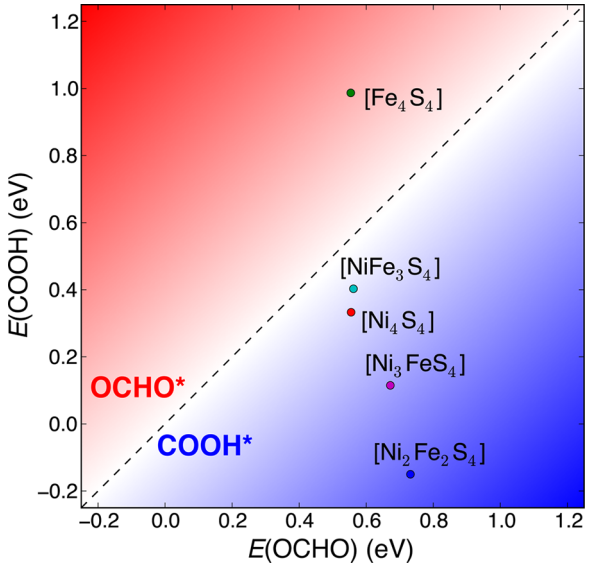

Figure 3. The calculated binding energies of the COOH* and OCHO* intermediates for the studied cubane compositions in the −2 charge state. The dashed line represents equal binding energies for the two intermediates and the crossover point between the pathways to produce HCOOH (top left) and CO (bottom right). All cubanes containing a Ni favor the COOH* intermediates and, thus, favor the formation of CO relative to HCOOH.

vs the OCHO* intermediates, that is, the descriptors for pathways favoring the formation CO or HCOOH, respectively. Assuming similar prefactors for the desorption processes on all cluster compositions, the substitution of a single Ni atom within the cubane results in reaction pathway for the formation of CO to become more preferable than the route to form HCOOH. This is in contrast to the full Fe cubane ($[Fe_4S_4]$), in which the route to HCOOH would be the first to open up, as seen from Figures 2 and 3. We find this to be the case for all cubanes containing at least one Ni, in which the COOH* intermediate is stabilized relative to the OCHO*. Thus, we find the structure of the cubanes to affect both the *activity* of electrochemical CO_2 to CO reduction, as well as the *selectivity*.

To compare more directly to other electrocatalysts, we plot our results for the Ni−Fe cubane systems on the proposed activity volcano for CO_2 electroreduction[9] in Figure 4. We note that we implicitly assume the same prefactors for COOH* formation when adsorbed on S in the cubanes as on the metals in ref 9. Of the 5 $[Ni_xFe_{4-x}S_4]$ (x = 0, ..., 4) cubane compositions, it can be seen that all of the Ni-containing clusters fall near or on the region of greatest predicted activity, whereas the cluster without Ni is not predicted to be active at all. The improved activity in the Ni-containing cubanes can be directly tied to the stabilization of the COOH* intermediate,

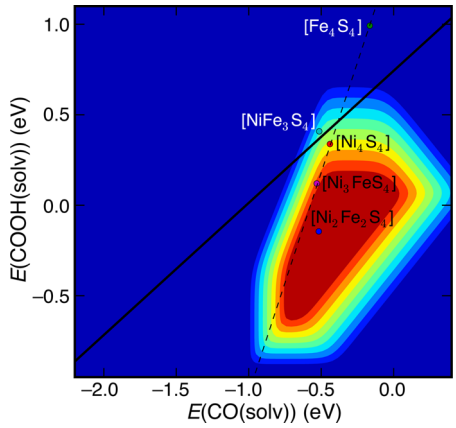

Figure 4. Kinetic volcano for CO evolution at 0.3 V overpotential from ref 9, where the height represents the CO evolution current. The solid line represents the trend line for the (211) step of transition metals, which does not pass over the top of the volcano. The dashed line represents the linear best fit of the $[Ni_xFe_{4-x}S_4]^{-2}$ (x = 0, ..., 4), which deviates significantly from the transition metals. Although the noble metals reside near the optimum of the trend line,[9] the cubanes containing at least one Ni are predicted to be comparably or much more active in the electroreduction of CO_2 to CO.

with the greatest stabilization in the $[Ni_2Fe_2S_4]^{-2}$ and $[Ni_3FeS_4]^{-2}$ clusters. We note that all of the Ni-containing cubanes are predicted to have activity comparable to or better than the best known metal catalysts,[9] as indicated by the transition metal scaling relation trend line in Figure 4. Furthermore, the cubanes exhibit their own distinct scaling relation (the dotted line in Figure 4), which passes closer to the more active regions of the predicted activity volcano. The unique scaling relation and the predicted activity enhancements suggest that these model cubane structures may be promising catalysts for improving the electroreduction of CO_2. Only experimental measurement will indicate whether this is observed in practice, as the stability of such structures is a critical concern.

To test the cluster stability, we considered dissociation events involving the removal of S in the form of desorbed H_2S and COS molecules and plotted the free energy of dissociation in Figure 5. We also consider alternate dissociation products in the Supporting Information, but find they are not as energetically favorable. The pathway to H_2S formation follows that of the hydrogen evolution reaction (HER), except that S is stripped from the cluster to produce H_2S rather than H_2. In Figure 5a, we show that this destructive reaction is more thermodynamically favorable for the clusters containing more than one Ni, whereas H_2 evolution is favored for the $[NiFe_3S_4]$ and $[Fe_4S_4]$ clusters. Similarly, in Figure 5b, we find that CO can also favorably strip away a S atom in clusters with more than 2 Ni, leading to the formation of COS. The $[Ni_2Fe_2S_4]$ cluster is found to be marginally unstable in the presence of CO at ambient conditions. This is particularly problematic for the CO_2 reduction pathway because we find the further protonation of COOH* would lead to CO* available to attack the cluster. The predicted instability of clusters containing more than one Ni may be indicative of why compositions with one or fewer Ni's are so widespread in nature, not the compositions with the greater predicted activities, such as $[Ni_2Fe_2S_4]$ or $[Ni_3FeS_4]$.

dx.doi.org/10.1021/cs4005419 | ACS Catal. 2013, 3, 2640−2643

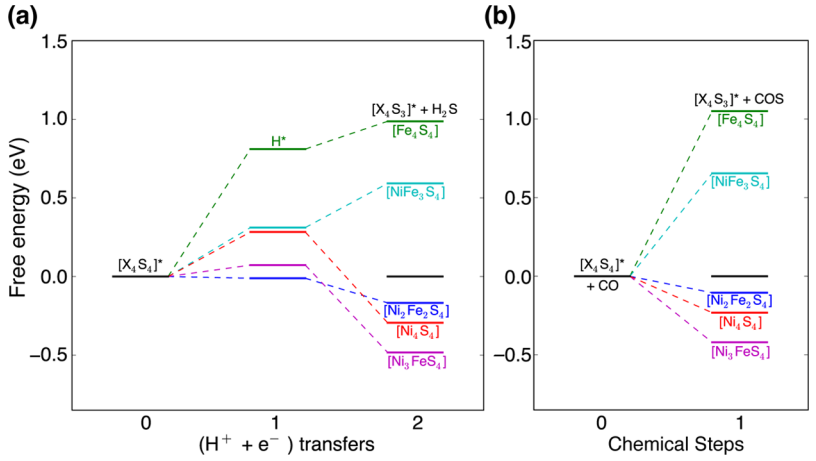

Figure 5. Free energy diagrams of possible cluster dissociation mechanisms shown for cubane compositions in the −2 charge state. (a) The H_2S pathway follows that for the HER for the first proton−electron transfer step but splits into to two distinct pathways for the second proton−electron transfer step. The black line shows the energy of producing H_2 and returning to the normal cluster composition ($[X_4S_4]$), whereas the other lines show the free energies of stripping a S atom from the cluster as H_2S, leaving a cluster of composition $[X_4S_3]$. (b) The COS pathway shows the free energies of CO + $[X_4S_4]$ clusters relative to a cluster of composition $[X_4S_3]$ and desorbed COS. Clusters with more than one Ni are found to generally favor the desorption of H_2S or COS under HER or CO_2 reduction conditions.

In conclusion, theoretical DFT calculations were performed on five cubane models inspired by the active site of the anaerobic Ni-CODH enzyme to ascertain the unique reactivity of the active site and the effect of the heteroatom substitution. The catalytic activity toward the reduction of CO_2 to CO and HCOOH on the cubanes was investigated for comparison with transition metal catalysts and Ni-CODH enzymes.[9] It was found that the substitution of Ni into the cubane lowered the energy pathway and improved the selectivity of all of the Ni-containing cubanes toward the formation of CO, as compared with the $[Fe_4S_4]$ cubane. For the $[Ni_xFe_{4-x}S_4]$ (x = 0, ..., 4) cubanes, we find the x = 2 and 3 clusters are predicted to be the most active according to the model of ref 9, and the cubanes containing one or four Ni's are predicted to be comparably active as the noble metals, the best known CO-producing pure metal surfaces. The cluster stability and dissociation of H_2S and COS was also assessed, in which only the cubanes with one or zero Ni were predicted to be stable under conditions facilitating hydrogen evolution and CO_2 reduction. These results give insight into unique structure−property relationships exhibited by cubanes of different compositions and also why naturally occurring $[Ni_xFe_{4-x}S_4]$ (x = 0, ..., 4) cubanes tend to have only one Ni.

■ ASSOCIATED CONTENT

Supporting Information

Details of the calculations, alternate dissociation pathways, and a summary of other charge states not presented in the main text. This material is available free of charge via the Internet at http://pubs.acs.org/.

■ AUTHOR INFORMATION

Corresponding Author

*E-mail: varley2@llnl.gov; norskov@stanford.edu.

Notes

The authors declare no competing financial interest.

■ ACKNOWLEDGMENTS

This work was supported by the Global Climate and Energy Project (GCEP) at Stanford University and the Catalysis for Sustainable Energy (CASE) initiative at the Technical University of Denmark, which is funded by the Danish Ministry of Science, Technology and Innovation. The Center for Atomic-Scale Materials Design (CAMd) is funded by the Lundbeck foundation.

■ REFERENCES

(1) Tester, J. W.; Drake, E. M.; Driscoll, M. J.; Golay, M. W.; Peters, W. A. *Sustainable Energy: Choosing Among Options*; MIT Press: Cambridge, MA, 2005.
(2) Hori, Y. *Modern Aspects of Electrochemistry*; Springer: New York, 2008.
(3) Kuhl, K. P.; Cave, E.; Abram, D. N.; Jaramillo, T. F. *Energy Environ. Sci.* **2012**, *5*, 7050−7059.
(4) Benson, E. E.; Kubiak, C. P.; Sathrum, A. J.; Smieja, J. M. *Chem. Soc. Rev.* **2009**, *38*, 89.
(5) Peterson, A. A.; Nørskov, J. K. *J. Phys. Chem. Lett.* **2012**, *3*, 251.
(6) Hori, Y.; Murata, A.; Kikuchi, K.; Suzuki, S. *J. Chem. Soc. Chem. Commun.* **1987**, 728−729.
(7) Parkin, A.; Seravalli, J.; Vincent, K. A.; Ragsdale, S. W.; Armstrong, F. A. *J. Am. Chem. Soc.* **2007**, *129*, 10328−10329.
(8) Ragsdale, S. W. *Crit. Rev. Biochem. Mol. Biol.* **2004**, *39*, 165−195.
(9) Hansen, H. A.; Varley, J. B.; Peterson, A. A.; Nørskov, J. K. *J. Phys. Chem. Lett.* **2013**, *4*, 388−392.
(10) Gu, W.; Seravalli, J.; Ragsdale, S. W.; Cramer, S. P. *Biochemistry* **2004**, *43*, 9029−9035.
(11) Dobbek, H.; Svetlitchnyi, V.; Liss, J.; Meyer, O. *J. Am. Chem. Soc.* **2003**, *126*, 5382−5387.
(12) Wong, G. B.; Bobrik, M. A.; Holm, R. H. *Inorg. Chem.* **1978**, *17* (3), 578−584.
(13) Henderson, R. A. *Chem. Rev.* **2005**, *105*, 2365−2437.